

BRIEF DEFINITIVE REPORT

An engineered concealed IL-15-R elicits tumor-specific CD8⁺T cell responses through PD-1-cis delivery

Jiao Shen^{1,2*}, Zhuangzhi Zou^{1,2*}, Jingya Guo¹, Yueqi Cai^{1,2}, Diyuan Xue³, Yong Liang³, Wenyan Wang³, Hua Peng¹, and Yang-Xin Fu³

Checkpoint blockade immunotherapy releases the inhibition of tumor-infiltrating lymphocytes (TILs) but weakly induces TIL proliferation. Exogenous IL-15 could further expand TILs and thus synergize with α PD-L1 therapy. However, systemic delivery of IL-15 extensively expands peripheral NK cells, causing severe toxicity. To redirect IL-15 to intratumoral PD-1⁺CD8⁺T effector cells instead of NK cells for better tumor control and lower toxicity, we engineered an anti-PD-1 fusion with IL-15-IL-15R α , whose activity was geographically concealed by immunoglobulin Fc region with an engineered linker (α PD-1-IL-15-R) to bypass systemic NK cells. Systematic administration of α PD-1-IL-15-R elicited extraordinary antitumor efficacy with undetectable toxicity. Mechanistically, cis-delivery of α PD-1-IL-15-R vastly expands tumor-specific CD8⁺T cells for tumor rejection. Additionally, α PD-1-IL-15-R upregulated PD-1 and IL-15R β on T cells to create a feedforward activation loop, thus rejuvenating TILs, not only resulting in tumor control in situ, but also suppressing tumor metastasis. Collectively, renavigating IL-15 to tumor-specific PD-1⁺CD8⁺T cells, α PD-1-IL-15-R elicits effective systemic antitumor immunity.

Introduction

Immune checkpoint blockade (ICB) therapy, such as anti-programmed cell death protein 1 (PD-1) and anti-PD-1 ligand 1 (α PD-L1) antibodies, releases the inhibition of tumor-infiltrating lymphocytes (TILs) and promotes the antitumor immunity (Scott et al., 2012; Sharpe and Pauken, 2018). Although PD-1/PD-L1-blockade immunotherapies induce durable and effective antitumor responses in patients with different types of advanced cancers, the complete response rate in clinical patients remains around 10–20% (Brahmer et al., 2012; Topalian et al., 2012). TILs play a vital role in antitumor immunity (Vilain et al., 2017). Even though PD-1/PD-L1 blockade could partially restore the cytotoxic function of T cells (Huang et al., 2017; Miller et al., 2019; Thommen and Schumacher, 2018), these cells often fail to expand and rapidly turn to dysfunctional status, leading to tumor relapse (Sakuishi et al., 2010). So, it is an emergent medical need to develop new approaches to both reinvigorate and expand dysfunctional TILs and reshape the immunosuppressive tumor microenvironment (TME) for effective cancer immunotherapies.

Cytokines are potent immune-modulating factors that can effectively expand immune cells, especially natural killer (NK)

and T cells (Xue et al., 2021). It is reported that the neutralization of endogenous cytokines, such as IL-2, abrogated the therapeutic effect of ICB (Garris et al., 2018; Hannani et al., 2015; Ren et al., 2022), suggesting an essential role of cytokines in immunotherapy. IL-2 is the first cytokine approved by FDA for metastatic renal cell cancer and advanced melanoma (Rosenberg, 2014). As a pleiotropic cytokine, IL-2 is potent at expanding NK and T cells. IL-2 treatment was also reported to decrease inhibitory receptor levels and increase the efficacy of PD-1 blockade (West et al., 2013). However, IL-2 could cause activation-induced cell death and the activation of immune inhibitory regulatory T cells (Treg cells; Lenardo, 1996). Additionally, excessive IL-2 in TME could also lead to T cell exhaustion and weak responsiveness to ICB therapy (Liu et al., 2021). Partially sharing IL-2's receptor IL-2R β (CD122) and C γ (CD132), IL-15 does not induce CD8⁺T cell exhaustion, activation-induced cell death, or Treg cells activation (Waldmann et al., 2020). Therefore, IL-15 is another potential cytokine for inducing potent antitumor immunity (Santana Carrero et al., 2019). IL-15 depletion corresponds with a high risk of tumor recurrence and reduced patient survival (Mlecnik et al., 2014).

¹Key Laboratory of Infection and Immunity, Institute of Biophysics, Chinese Academy of Sciences, Beijing, China; ²University of Chinese Academy of Sciences, Beijing, China; ³Department of Basic Medical Sciences, School of Medicine, Tsinghua University, Beijing, China.

*J. Shen and Z. Zou contributed equally to this paper. Correspondence to Yang-Xin Fu: Yangxinfu@tsinghua.edu.cn; Hua Peng: hpeng@moon.ibp.ac.cn.

© 2022 Shen et al. This article is distributed under the terms of an Attribution-Noncommercial-Share Alike-No Mirror Sites license for the first six months after the publication date (see <http://www.rupress.org/terms/>). After six months it is available under a Creative Commons License (Attribution-Noncommercial-Share Alike 4.0 International license, as described at <https://creativecommons.org/licenses/by-nc-sa/4.0/>).

A previous study has reported an IL-15/IL-15R α complex named IL-15 superagonist (sIL-15) that greatly enhances IL-15 bioactivity (Rubinstein et al., 2006). However, systemic administration of sIL-15 leads to extensive peripheral lymphocyte expansion and acute lymphocytic pneumonitis (Guo et al., 2021; Ochoa et al., 2013). As one of the most famous designs, N-803 encompassing IL-15/IL-15R α and Fc is currently under investigation for safety and toxicity in several Phase I clinical trials (Fiore et al., 2020; Rhode et al., 2016). Intravenous injection of N-803 achieved clearance of lung metastasis in two patients with hematologic malignancies relapsing after allogeneic hematopoietic cell transplantation (Romee et al., 2018). However, NK-targeted N-803 increases NK proliferation by up to 14-fold change in peripheral blood, which may lead to NK-dependent toxicity (Margolin et al., 2018). Several studies also show that repeated injection of N-803 may reduce biological responsiveness in macaque and patients with metastatic non-small cell lung cancer (Ellis-Connell et al., 2018; Wrangle et al., 2018). Much effort has been spent on targeting sIL-15 in tumor tissues by antibodies to tumor-associated antigens (Beha et al., 2019; Jochems et al., 2019; Knudson et al., 2020; Liu et al., 2020; Liu et al., 2018; Martomo et al., 2020; Vincent et al., 2013). Nevertheless, the lack of tumor-specific antigen and high affinity of IL-15 for its receptors may result in an “on-target” but “off-tumor” effect (Stoklasek et al., 2006). Thus IL-15 cannot be targeted to tumors effectively. Besides, tumor cells might internalize those fusion proteins and limit their targeting to T cells. Researchers recently tried to mutate cytokines to weaken binding affinity for their receptors and reduce peripheral consumption (Ren et al., 2022; Shen et al., 2020; Xu et al., 2021). However, some mutations might influence the stability of cytokines and be more likely to induce anticytokine antibodies. Generally, toxicity reduction is at the cost of losing activity caused by mutations. Decreasing toxicity while maintaining efficacy is the pending dilemma of cytokine application. Here, instead of mutation, we used the Fc domain of α PD-1 antibody to conceal super IL-15 binding to the IL-15R β , physically achieved by a delicate linker design between Fc and super IL-15. Intriguingly, α PD-1 antibody not only anchored the concealed sIL-15 on PD-1⁺CD8⁺T cells directly but also exposed sIL-15 activity to these cells. Thus, we developed a next-generation IL-15-based immuno-cytokine, α PD-1-concealed sIL-15 (α PD-1-IL-15-R), targeting and anchoring IL-15 on the intratumoral PD-1⁺CD8⁺T cells to release the complete sIL-15 function via cis-delivery.

Result

Construction of a concealed sIL-15 to reduce peripheral consumption and toxicity

The blockade of PD-1/PD-L1 could release the inhibition on T cells, and additional IL-15 could promote T cell activation and proliferation. Thus we proposed to take advantage of PD-1/PD-L1 and IL-15 to synergize the T cell responses. We first combined sIL-15 with α PD-L1 for MC38 tumor treatment and found that the combination therapy exhibited a better anti-tumor effect than sIL-15 or α PD-L1 alone (Fig. 1 A). However, the sIL-15 treatment alone indeed caused severe weight loss,

even at the dose that merely achieves limited antitumor activity (Fig. 1 B).

To determine the major cell subsets that contribute to severe side effects, we evaluated IL-15R β expression in peripheral blood mononuclear cells and tumor tissues. We found that NK cells express much higher IL-15R β than both CD4⁺T cells and CD8⁺T cells in peripheral blood mononuclear cells and tumor tissues (Fig. 1 C and Fig. S1 A). According to the in vitro binding of IL-15 to the splenocytes, this high expression of IL-15R β may lead most IL-15 to NK cells (Fig. S1 B). Depleting NK cells during sIL-15 treatment failed to change antitumor activity but prevented huge weight loss and death (Fig. S1, C-E). These results suggested that NK cells are mainly responsible for sIL-15-induced toxicity rather than antitumor effects. Therefore, reducing IL-15R β binding affinity is required to ameliorate the NK-dependent toxicity of the IL-15. Based on the structure of the IL-15 quaternary complex (4GS7), several amino acids (S7, K10, K11) in the N-terminal domain of IL-15 are the determinants for the interaction with its receptor (Ring et al., 2012; Fig. S1 F). Thus, we proposed that IL-15 binding for IL-15R β could be physically concealed by fusing the hIgG1 immunoglobulin Fc domain at the N-terminus of IL-15 when its C-terminus links to IL-15R α . We designed and constructed Fc-IL-15R α -IL-15 (R-IL-15) and Fc-IL-15-IL-15R α (IL-15-R) fusion proteins to test our hypothesis (Fig. 1 D). Fc domain was used to prolong the half-life of IL-15 besides the potential function block. The length of the linker between IL-15 and IL-15R α was constant to maintain the high activity of the IL-15/IL-15R α complex. Linkers with variable length between Fc and IL-15/IL-15R α complex were designed and analyzed for the functional concealment of sIL-15 by Fc. First, we assessed the IL-15 activity of fusion proteins using a CTLL-2 reporter cell line. We found that compared with R-IL-15, the activity of IL-15-R was blocked entirely. By gradually extending the linker length (from G₄S to [G₄S]₃) between Fc and IL-15, the sIL-15 activity was gradually recovered. This result suggested that the link length might also be dictated to the extent of blocking (Fig. 1 E). The high binding affinity of sIL-15-Fc on NK cells was abrogated entirely in IL-15-R (Fig. S1 B). This phenomenon confirmed our hypothesis that the Fc domain could nicely conceal the sIL-15 binding affinity for its receptor. During systemic administration in mice bearing MC38 tumors, IL-15-R did not cause weight loss, whereas R-IL-15 still induced severe toxicity (Fig. 1, F and G; and Fig. S1 G). R-IL-15 produced more lymphocytes and inflammatory cytokines in the peripheral, contributing to the lethal toxicity (Fig. 1, H and I; and Fig. S1 H), suggesting a possible need to block IL-15 at both N- and C-termini.

α PD-1-IL-15-R achieves potent antitumor effects and reduces toxicity via targeting sIL-15 to intratumoral CD8⁺T cells

Based on the synergistic effect of sIL-15 with ICB, we selected the α PD-1 and the α PD-L1 antibody that not only delivers IL-15 to TME but also releases the checkpoint inhibition on TILs. First, we investigated PD-1 and PD-L1 expression on immune cells in several tissues. It has been reported that the expression of PD-L1 is lower in tumors than in draining lymph nodes (dLNs). Besides, dendritic cells (DCs) and M ϕ within the tumor express

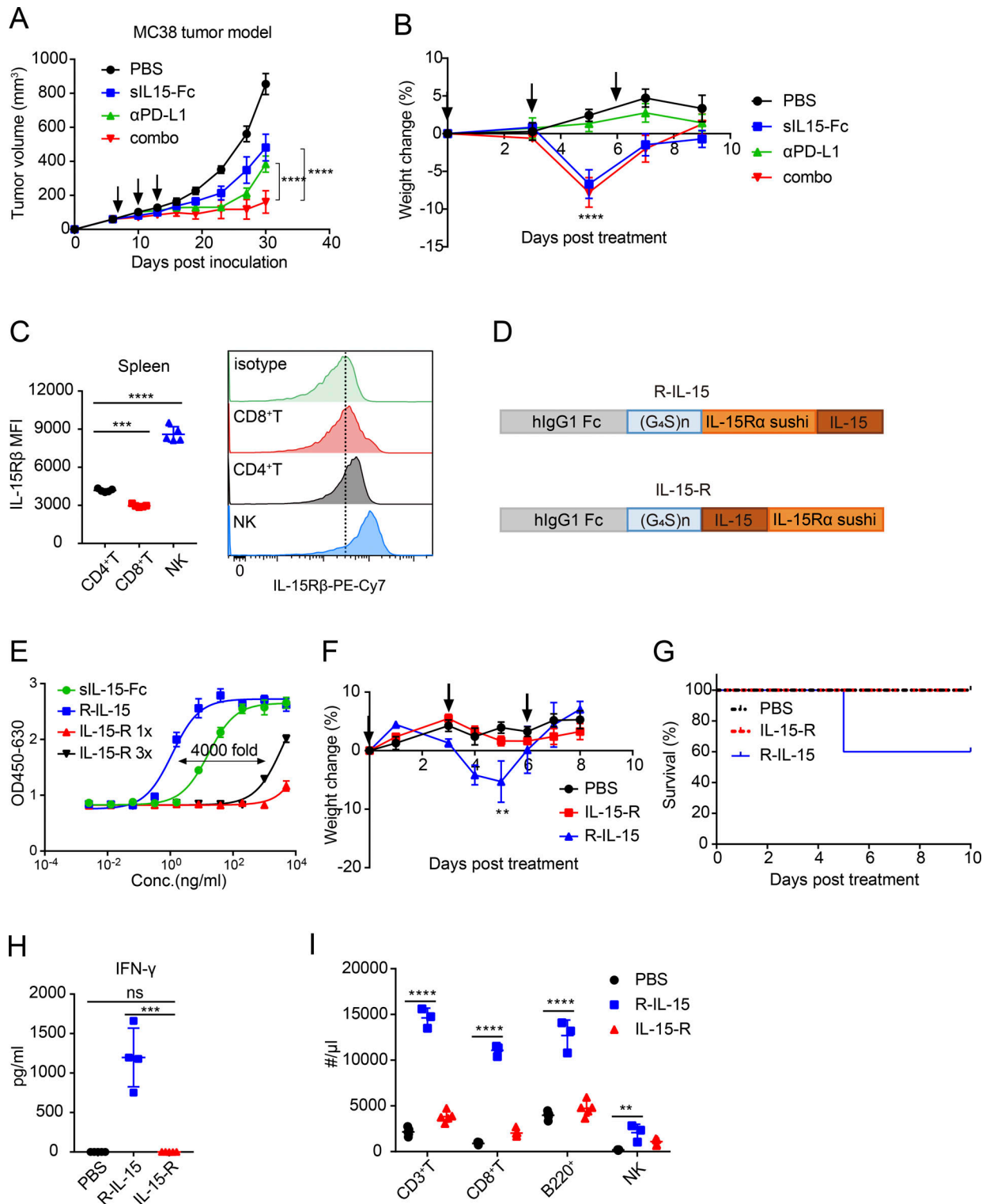


Figure 1. The engineering of a concealed sIL-15 with negligible toxicity. (A and B) C57BL/6 mice ($n = 5$) were inoculated with 5×10^5 MC38 cells. Tumor-bearing mice were intraperitoneally treated with PBS or 15 μ g sIL-15-Fc or 50 μ g α PD-L1 or the combination of 15 μ g sIL-15-Fc and 50 μ g α PD-L1 on days 7, 10, and 14. Tumor volume (A) and body weight (B) were measured as indicated. (C) Spleens were collected from tumor-bearing mice 14 d after the inoculation. Cells were isolated and stained for flow cytometric analysis. (D) Schematic diagram of R-IL-15 and IL-15-R. (E) The bioactivity of the indicated proteins was detected by the proliferation of the CTLL-2 reporter cell line. IL-15-R 1x or IL-15-R 3x represented one or three G_4S linkers between Fc and IL-15. Conc., concentration. (F and G) C57BL/6 mice ($n = 5$) were inoculated with 5×10^5 MC38 cells. Tumor-bearing mice were intraperitoneally treated with PBS or 15 μ g IL-15-R or R-IL-15 on days 7, 10, and 13. Body weight (F) and survival (G) were measured as indicated. (H and I) The mice were treated as shown in F. IFN- γ from the serum (H) was measured 6 h after the second injection by a cytometric bead assay. Certain cell types (I) from peripheral blood were collected 48 h after the second injection and counted by flow cytometric analysis. Data are shown as mean \pm SEM from two to three independent experiments. The P value was determined by two-way ANOVA with Geisser–Greenhouse’s correction (A–C, F, H, and I). ** $P < 0.01$, *** $P < 0.001$, **** $P < 0.0001$.

higher PD-L1 than CD45⁻ tumor cells (Tang et al., 2018; Fig. S2 A). We found that α PD-L1-IL-15-R bound PD-L1 expressing MC38 tumor cells in vitro efficiently (Fig. S2 B). But it might inefficiently bind MC38 tumor cells in vivo in the presence of other PD-L1 high expressing cells, such as DC, M ϕ , or myeloid-derived suppressor cells (MDSCs) in dLNs. Thus, we proposed that PD-L1 might not be suitable for tumor targeting. However, we found that CD8⁺T cells expressed a higher PD-1 level than CD4⁺T cells and NK cells in the tumor; meanwhile, CD8⁺T cells in other tissues barely expressed PD-1 (Fig. 2, A and B; and Fig. S2 C). Interestingly, NK cells within the tumor expressed the highest level of IL-15R β (Fig. S1 A) but the lowest level of PD-1 (Fig. 2 A). Therefore, we proposed that PD-1 might be an ideal targeting molecule to renavigate IL-15-R toward intratumoral CD8⁺T cells rather than NK cells. To evaluate that, we generated a fusion protein α PD-1-IL-15-R (Fig. 2 C). This protein comprised an engineered IL-15-R led by a high-affinity α PD-1 Fab homodimer antibody. To verify the importance of sIL-15 activity concealing, α PD-1-R-IL-15 was generated as toxicity control. The purity of the proteins was verified by SDS-PAGE (Fig. S2 D). To verify the role of α PD-1, we incubated α PD-1-IL-15-R with tumor tissue in vitro. This result indicated that α PD-1 could preferentially deliver IL-15-R to PD-1-expressing CD8⁺T cells rather than CD4⁺T cells or NK cells (Fig. 2, D and E). To investigate the role of α PD-1 in facilitating IL-15-R binding, we engineered a CTLL-2 reporter cell line that expressed mouse PD-1 stably (Fig. S2 E). Compared to CTLL-2, α PD-1-IL-15-R reacquired IL-15 activity as vigorous as R-IL-15 in PD-1 expressing CTLL-2 (Fig. 2 F). This result confirmed that IL-15-R could firmly contact IL-15R β with the help of PD-1 anchoring, resulting in fully recovered IL-15 activity. More importantly, we performed a “cis or trans” assay by coculturing α PD-1-IL-15-R with the mixture of CTLL-2 WT and CTLL-2-mPD1. CTLL-2 WT and CTLL-2-mPD1 cells were labeled with cell trace violet and CFSE, respectively. The phosphorylation of the STAT-5 signal was detected. If via in cis delivery, α PD-1 and IL-15-R, the two functional units of the fusion protein should be delivered on the same receptor-expressing cells, and if via in trans delivery, the fusion protein may deliver its separate function on the different receptor-expressing cells. We found that the IL-15 stimulated pSTAT-5 signal could only be detected on PD-1 expressing cells (Fig. 2 G). This result revealed that the concealed IL-15 part was delivered to IL-15 receptors in cis via binding to the PD-1 expressed on the CTLL-2-mPD1 cells but not in trans on the cocultured CTLL-2 WT cells. To determine if α PD-1-IL-15-R can target tumor tissue in vivo, we intravenously injected this fusion protein into the tumor-bearing mice and collected various tissues and tumors 24 h later. The in vivo biodistribution of α PD-1-IL-15-R displayed specific retention in tumors rather than normal tissues (Fig. 2 H). Together, α PD-1-IL-15-R can preferentially bind to intratumoral PD-1⁺CD8⁺T cells but not peripheral PD-1⁻ immune cells.

We then analyzed α PD-1-IL-15-R antitumor activity and toxicity in vivo. We first treated the MC38 colon tumor at an early stage (day 7). Strikingly, α PD-1-IL-15-R exhibited an excellent antitumor effect without any weight loss during the entire treatment. However, all mice experienced severe weight

loss and even died after only the second dose of α PD-1-R-IL-15 (Fig. 3, A–C). We also compared the antitumor effect between α PD-1 and α PD-L1 fused with IL-15-R to test the advantage of cis versus trans delivery in vivo. The inferior antitumor efficacy of α PD-L1-IL-15-R confirmed our hypothesis that α PD-L1 is unsuitable for delivering IL-15-R (Fig. S2 F). During the clinical application of IL-15, cytokine release syndrome always leads to severe toxicity and poor prognosis (Robinson and Schluns, 2017). To further evaluate the safety of α PD-1-IL-15-R, we examined the serum inflammatory cytokines. Compared with α PD-1-R-IL-15, α PD-1-IL-15-R displayed an undetectable level of TNF, IFN- γ , and MCP-1 (Fig. 3 D).

α PD-1-IL-15-R provides potent antitumor immunity through cis-delivery of IL-15 activity

To explore the importance of PD-1 targeting, we compared α PD-1-IL-15-R with the combination therapy of α PD-1 mixed with IL-15-R. At a low dose, the α PD-1 and IL-15-R combination showed no tumor control (Fig. 3 E). Only at a high dose (200 μ g) could α PD-1 partly control the tumor growth. However, α PD-1-IL-15-R exhibited better antitumor efficacy even than high dose α PD-1, and this effect was abrogated after the neutralization of IL-15R β (Fig. S2 G). These results suggested that α PD-1 as a part of α PD-1-IL-15-R could partly function as a checkpoint inhibitor at a 10-fold less dosage than α PD-1 alone treatment. More importantly, we found that the antitumor effect of α PD-1-IL-15-R at a low dose could be further enhanced by extending the linker between the Fc domain and IL-15 (from G₄S to [G₄S]₃). To study if PD-1 is required, we first compared α PD-1-IL-15-R with α EGFR-IL-15-R, two molecules with the same linker and design except for different antibodies. The α PD-1-IL-15-R with (G₄S)₃ had a significant antitumor effect even in advanced tumors (day 14), while α EGFR-IL-15-R with (G₄S)₃ did not, which demonstrated an indispensable role of α PD-1 in tumor control (Fig. 3 F). To characterize the antitumor efficacy of α PD-1-IL-15-R for different tumor models, we treated A20 and B16F10 tumor-bearing mice with α PD-1-IL-15-R and observed that α PD-1-IL-15-R displayed great antitumor effects in both tumor models (Fig. 3, G and H). These data demonstrated that the α PD-1-IL-15-R has a potent antitumor effect in multiple types of tumor models.

To further assess whether α PD-1-IL-15-R delivered IL-15-R to the IL-15R β on the PD-1 targeting T cells through cis delivery in vivo, we separated PD-1's function as targeting and anchoring IL-15-R. We constructed α EGFR-IL-15-R and generated MC38-EGFR5 tumor, expressing mutant mouse EGFR for effective binding by α EGFR (human) Fab. An equal molar of α PD-1 was additionally injected into the α EGFR-IL-15-R treatment group to provide the α PD-1 signal. Although α EGFR-IL-15-R can target MC38-EGFR5 tumor cells, the antitumor effect of α EGFR-IL-15-R was significantly lower than that of α PD-1-IL-15-R, indicating that tumor cell targeting, but not effector cell targeting, was insufficient for IL-15 activity recovery (Fig. 3 I). Besides, we also tested the antitumor efficacy in a humanized tumor model. We found that α PD-1-IL-15-R could effectively control tumor growth (Fig. 3 J). Collectively, these data suggested that α PD-1-IL-15-R could target tumor tissues, anchor, and cis-deliver IL-15 on PD-1⁺ TILs to achieve the best therapeutic effect.

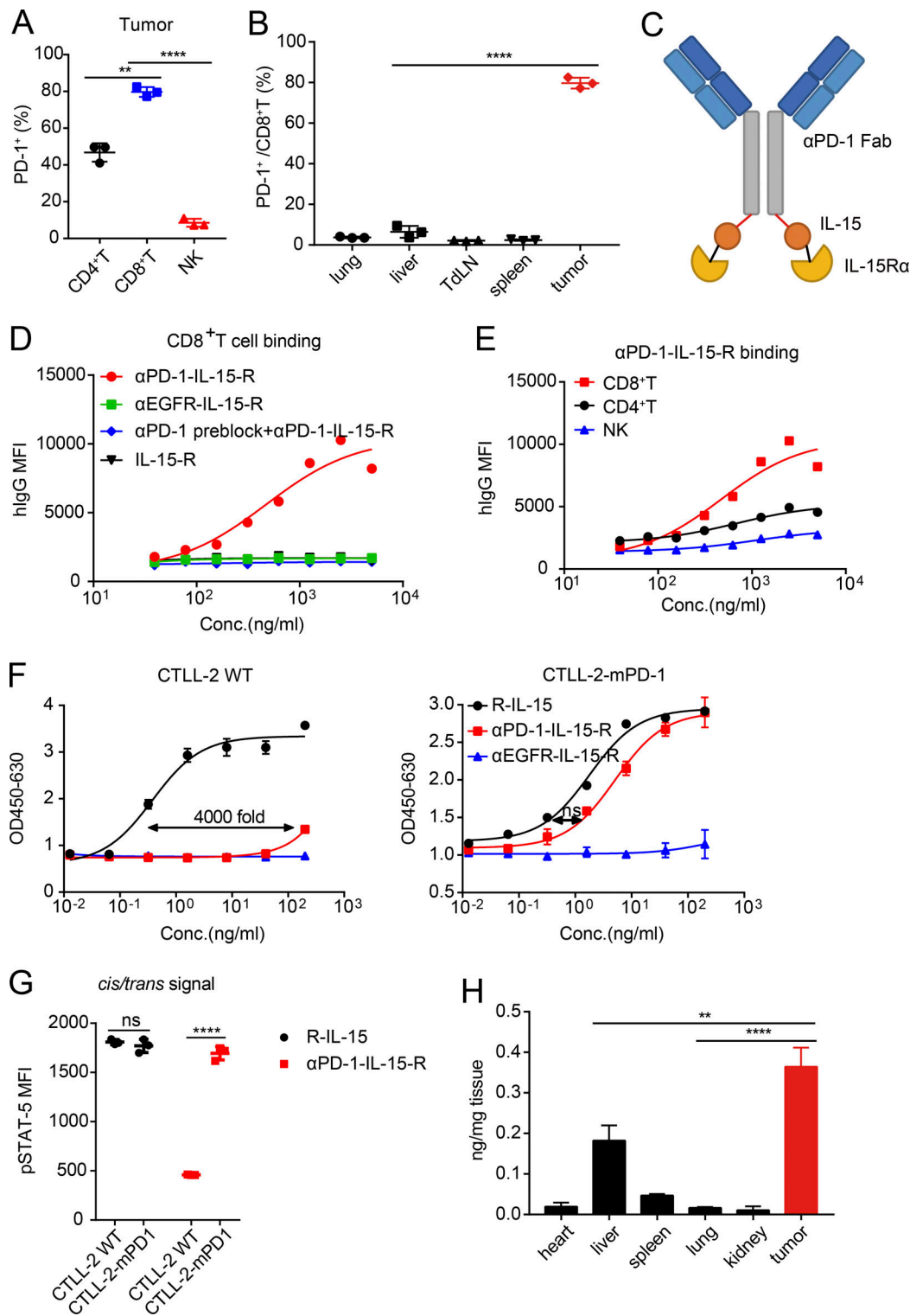


Figure 2. PD-1 navigates concealed sIL-15 to intratumoral CTLs through cis-delivery. (A and B) C57BL/6 mice were inoculated with 5×10^5 MC38 cells, and tissues (lung, liver, dLN, spleen, and tumor) were collected. PD-1 level of CD4⁺T, CD8⁺T, NK cells from the tumor (A), and CD8⁺T cells from the indicated tissues (B) was measured by flow cytometric analysis. (C) Schematic diagram of αPD-1-IL-15-R. (D and E) MC38 tumor-bearing mice were sacrificed, and tumor tissue was collected. Different proteins, as indicated, were incubated with the tumor tissue suspension. Protein binding with CD4⁺T, CD8⁺T, and NK cells was detected by flow cytometric analysis. MFI, mean fluorescence intensity. (F) The bioactivity of the indicated proteins was detected by the proliferation of WT CTLL-2 and engineered CTLL-2-mPD-1 reporter cell line. (G) CTLL-2-mPD1 was labeled with CFSE, and CTLL-2 WT was labeled with cell trace violet. R-IL-15 or αPD-1-IL-15-R was incubated with a mixture of labeled cells for 30 min. The pSTAT-5 level was detected by flow cytometry on CTLL-2 WT and engineered CTLL-2-mPD1 reporter cell line. (H) MC38 tumor-bearing mice ($n = 3$) were intravenously injected with 5 μg αPD-1-IL-15-R and sacrificed after 24 h. Mice tissues were collected and homogenized. The concentration of the fusion protein in the supernatant was measured and normalized by ELISA. Data are shown as mean ± SEM from two to three independent experiments. The P value was determined by two-way ANOVA with Geisser–Greenhouse’s correction (A, B, G, and H). ** $P < 0.01$, **** $P < 0.0001$.

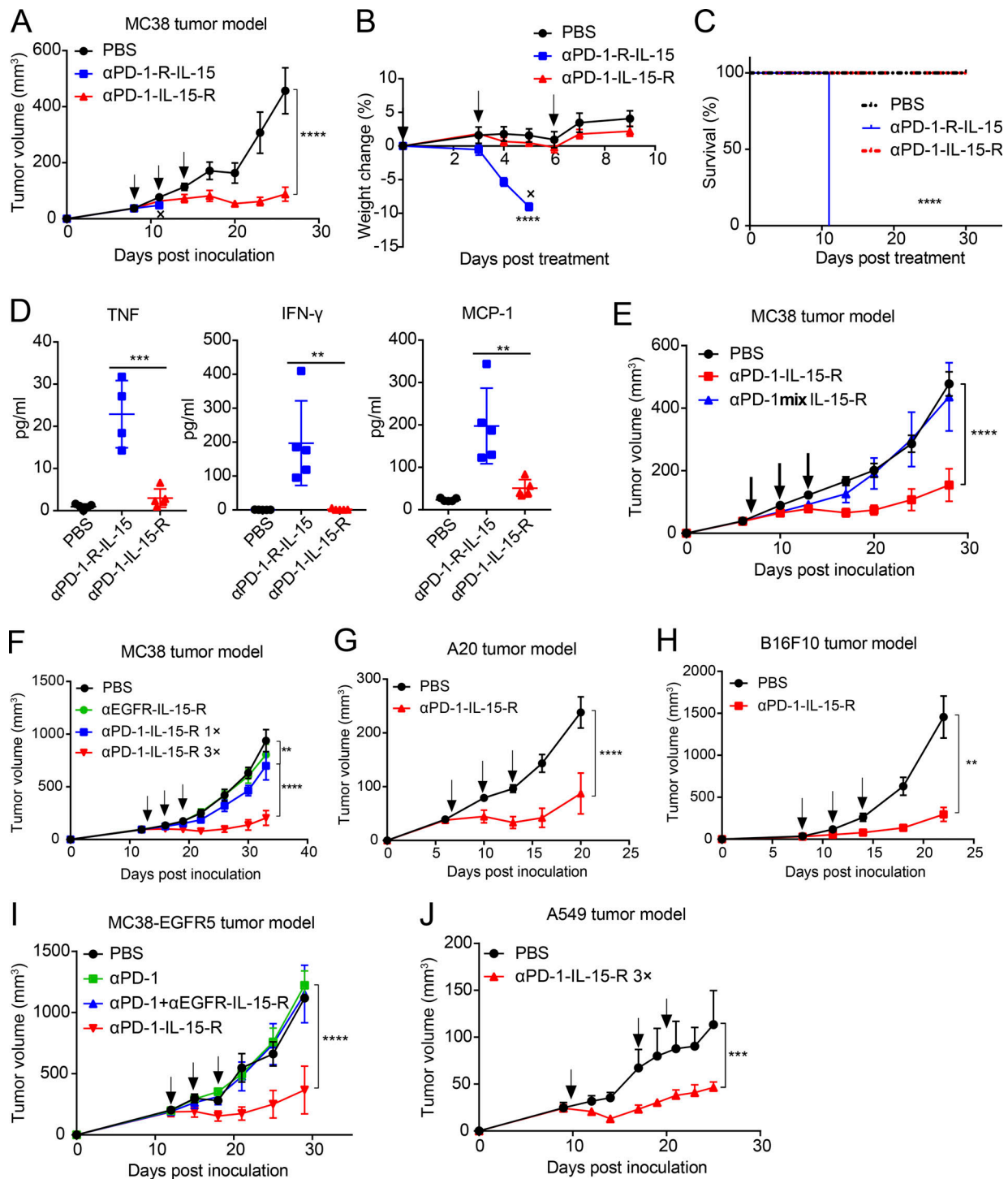


Figure 3. PD-1-IL-15-R cis-delivery dramatically enhances antitumor immunity while reducing toxicity. (A–C) C57BL/6 mice ($n = 5$) were inoculated with 5×10^5 MC38 cells. Tumor-bearing mice were intraperitoneally treated with PBS or $30 \mu\text{g}$ αPD-1-IL-15-R or αPD-1-R-IL-15 on days 7, 10, and 13. Tumor volume (A), body weight (B), and survival (C) were measured as indicated. (D) C57BL/6 mice ($n = 5$) were treated as shown in A. Blood was collected 6 h after the second injection. TNF, IFN- γ , and MCP-1 in the serum were measured by a cytometric bead assay. (E) C57BL/6 mice ($n = 5$) were inoculated with 5×10^5 MC38 cells. Tumor-bearing mice were intraperitoneally treated with PBS or $30 \mu\text{g}$ αPD-1-IL-15-R or the mix of equimolar αPD-1 Fab and IL-15-R on days 7, 10, and 13. Tumor volume was measured as indicated. (F) C57BL/6 mice ($n = 5$) were inoculated with 5×10^5 MC38 cells. Tumor-bearing mice were intraperitoneally treated with PBS or $30 \mu\text{g}$ αEGFR-IL-15-R or αPD-1-IL-15-R with different linker lengths (G_4S or $[G_4S]_3$) on days 14, 17, and 20. Tumor volume was measured as indicated. αPD-1-IL-15-R 1x or αPD-1-IL-15-R 3x represented one or three G_4S linker between αPD-1 and IL-15. (G) Balb/c mice ($n = 5$) were inoculated with 5×10^6 A20 cells. Tumor-bearing mice were intraperitoneally treated with PBS or $30 \mu\text{g}$ αPD-1-IL-15-R on days 7, 10, and 13. Tumor volume was measured as indicated. (H) C57BL/6 mice ($n = 5$) were inoculated with 3×10^5 B16F10 cells. Tumor-bearing mice were intraperitoneally treated with PBS or $30 \mu\text{g}$ αPD-1-IL-15-R on days 8, 11, and 14. Tumor volume was measured as indicated. (I) C57BL/6 mice ($n = 5$) were inoculated with 5×10^5 MC38-EGFR5 cells. Tumor-bearing mice were intraperitoneally treated with PBS or $15 \mu\text{g}$ αPD-1 or $30 \mu\text{g}$ αEGFR-IL-15-R or $30 \mu\text{g}$ αPD-1-IL-15-R on days 14, 17, and 20. Tumor volume was

measured as indicated. (J) CD34⁺ humanized mice ($n = 3$) were inoculated with 2×10^6 A549 cells. Tumor-bearing mice were intraperitoneally treated with PBS or α PD-1-IL-15-R with three G₄S as a linker between α PD-1 and IL-15 on days 10 (10 μ g), 17 (20 μ g), and 20 (20 μ g). Tumor volume was measured as indicated. Data are shown as mean \pm SEM from two to three independent experiments. The P value was determined by two-way ANOVA with Geisser–Greenhouse’s correction (A, B, and D–J) or a log-rank test (C). **P < 0.01, ***P < 0.001, ****P < 0.0001.

α PD-1-IL-15-R selectively activates and expands PD-1⁺ tumor-specific CD8⁺T cells

To explore which individual cell types are responsible for the antitumor efficacy of α PD-1-IL-15-R on the MC38 tumor model, we first used *Rag1*^{-/-} mice that lack adaptive immunity. The antitumor effect was entirely abrogated in *Rag1*^{-/-} mice (Fig. 4 A). Then we depleted NK cells, CD4⁺T cells, or CD8⁺T cells by respective depletion antibodies. When NK cells or CD4⁺T cells were depleted, the antitumor efficacy of α PD-1-IL-15-R was barely affected, further confirming that CD4⁺T cells or NK cells were insufficient for tumor control (Fig. S3, A and B). However, the depletion of CD8⁺T cells completely abolished the antitumor efficacy (Fig. 4 B). To determine whether IFN- γ contributes to the α PD-1-IL-15-R-mediated antitumor effect, we treated MC38 tumor-bearing mice with IFN- γ neutralizing antibody during α PD-1-IL-15-R treatment. We observed an abrogated antitumor effect, indicating IFN- γ played an essential role in antitumor immunity (Fig. 4 C). Together, we proved that CD8⁺T cells but not NK or CD4⁺T cells contributed to the tumor control through IFN- γ .

As CD8⁺T cells were essential for α PD-1-IL-15-R-induced tumor control, we further investigated the nature of the CD8⁺T cell response to α PD-1-IL-15-R treatment. We found that the percentage and quantity of CD8⁺T cells were increased within the tumor after the treatment (Fig. 4 D). Interestingly, the total cell number of the PD-1⁺CD8⁺ T cell subset was increased dramatically (Fig. S3 C). To investigate where this PD-1⁺CD8⁺ T cell subset came from, we examined Ki-67 expression, a cell-proliferation marker, in PD-1⁺CD8⁺T cells. After the α PD-1-IL-15-R treatment, more PD-1⁺CD8⁺T cells expressed Ki-67 (Fig. S3 D). Additionally, the number of IFN- γ ⁺PD-1⁺CD8⁺T cells also significantly increased (Fig. 4 E). Although we have confirmed that α PD-1-IL-15-R targets tumor tissue and intratumoral PD-1⁺CD8⁺T cells, it was not clear if this subset of T cells plays a full part in tumor control. To explore whether intratumoral CD8⁺T cells are enough for the antitumor effect, we treated mice with FTY720 1 d before the α PD-1-IL-15-R therapy to block T cells egressing from LNs. FTY720 is a small-molecule analog of sphingosine 1-phosphate. FTY720 could internalize and degrade the sphingosine 1-phosphate receptor, preventing lymphocyte egressing from the LNs. Interestingly, α PD-1-IL-15-R could still effectively control tumors in tumor-bearing mice treated with FTY720, which suggested that pre-existing T cells within the tumor were sufficient for tumor control (Fig. 4 F).

We also performed a tetramer assay to track tumor-specific CD8⁺T cells in the MC38-OVA tumor model. The increased quantity of OVA⁺CD8⁺T cells indicated that α PD-1-IL-15-R could proliferate tumor-specific CD8⁺T cells (Fig. 4 G). To confirm whether α PD-1-IL-15-R can enhance the function of tumor-specific CD8⁺T cells, we sorted the tetramer⁻ and tetramer⁺ CD8⁺T cells from the tumor tissues of MC38-OVA tumor-

bearing mice and incubated these cells with α PD-1-IL-15-R in vitro. Impressively, we found α PD-1-IL-15-R could induce much higher IFN- γ production of tetramer⁺ CD8⁺T cells, suggesting that α PD-1-IL-15-R preferred to invigorate tumor-specific T cells (Fig. 4 H). Collectively, these data demonstrated that α PD-1-IL-15-R enhanced antitumor immunity through the preferential proliferation of tumor-specific PD-1⁺CD8⁺T cells.

To understand how α PD-1-IL-15-R regulates CD8⁺T cell function in vivo, we performed an RNA-sequencing (RNA-seq) analysis of the intratumoral CD8⁺T cell sorted from MC38 tumors treated with or without α PD-1-IL-15-R. Gene set enrichment analysis revealed strong pathway enrichment and gene expression of immune response-associated biological processes, such as T cell differentiation, T cell activation, and cytolysis (Fig. 4 I). Additionally, these CD8⁺T cells from mice treated with α PD-1-IL-15-R exhibited higher expression levels of genes representing T cell differentiation, such as *Tcf-7*, *Mki67*, and *Ly6c2*, and those genes representing cytotoxic function, such as *Gzmb*, *Tnf*, and *Prfl* (Fig. 4, J and K; and Fig. S3 E). Notably, the expression of *pdcd1* and *Il2rb* was upregulated after α PD-1-IL-15-R treatment (Fig. 4 K). This phenomenon suggested that α PD-1-IL-15-R may provide a positive feedback loop, further increasing the efficacy of α PD-1-IL-15-R treatment. Altogether, these data indicated that α PD-1-IL-15-R treatment reinvigorated tumor-specific CD8⁺T cells with enhanced proliferative and cytotoxic functions.

α PD-1-IL-15-R controls cold tumors and metastatic tumors

Turin-Bologna (TUBO) tumor model derived from the transgenic BALB/c mice with the *neu* oncogene is a HER2/*neu*-dependent mammary carcinoma. TKI therapy (tyrosine kinase inhibitor) can temporarily control the TUBO tumor, but the tumor would finally relapse. Thus, we proposed that TKI could increase the infiltration of TILs, and α PD-1-IL-15-R could expand and invigorate TILs to overcome TKI resistance. In this experiment, we used a second-generation TKI (afatinib) to treat the mice with established tumors and observed tumor relapse in all the mice. However, TKI, in combination with α PD-1-IL-15-R, could effectively control tumor growth (Fig. 5 A). Together, these findings suggested that α PD-1-IL-15-R can overcome TKI resistance and control poor immunogenic tumors.

Tumor metastasis is the clinic’s primary cause of treatment failure and cancer-related life-threatening diseases. We first assessed whether α PD-1-IL-15-R could induce a protective memory response. Cured mice were injected with five times the original tumor cells on the same site after eliminating the tumors, and all mice rejected the rechallenged tumors and survived (Fig. 5, B and C). Thus, we proposed that α PD-1-IL-15-R as a neoadjuvant protocol could provide long-term protection to overcome tumor metastasis. We then subcutaneously inoculated the B16F10 tumor cells and intravenously injected the B16F10

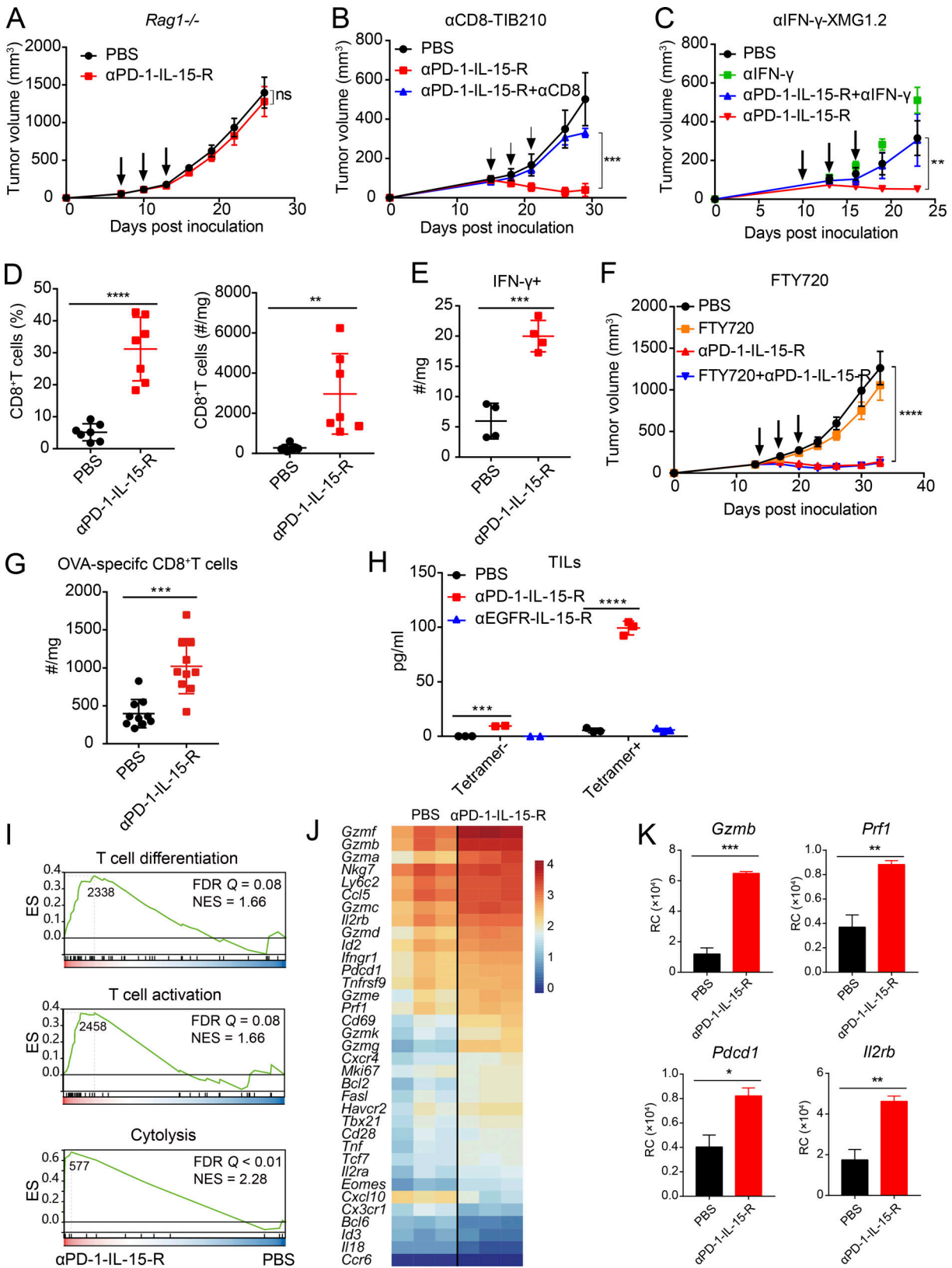


Figure 4. **αPD-1-IL-15-R activates and expands PD-1⁺ tumor-specific CD8⁺T cells.** (A) *Rag1*^{-/-} mice (n = 5) were inoculated with 5 × 10⁵ MC38 cells. Tumor-bearing mice were intraperitoneally treated with PBS or 30 μg αPD-1-IL-15-R on days 7, 10, and 13. Tumor volume was measured as indicated. (B) C57BL/6 mice (n = 5) were inoculated with 5 × 10⁵ MC38 cells. Tumor-bearing mice were intraperitoneally treated with PBS or 30 μg αPD-1-IL-15-R on days 7, 10, and 13. For cell depletion, mice were injected with 200 μg αCD8 antibody on the same day. Tumor volume was measured as indicated. (C) C57BL/6 mice (n = 5) were inoculated with 5 × 10⁵ MC38 cells. Tumor-bearing mice were intraperitoneally treated with PBS or 30 μg αPD-1-IL-15-R on days 7, 10, and 13. For IFN-γ

neutralization, mice were injected with 500 μg $\alpha\text{-IFN-}\gamma$ antibody on the same day. Tumor volume was measured as indicated. **(D and E)** C57BL/6 mice ($n = 4\text{--}7$) were inoculated with 5×10^5 MC38 cells. Tumor-bearing mice were intratumorally treated with PBS or 30 μg $\alpha\text{PD-1-IL-15-R}$ on days 14 and 17. The mice were sacrificed, and tumor tissues were collected 48 h after the second injection. The number and percentage of intratumoral CD8⁺T cells (D) and the number of IFN- γ ⁺PD-1⁺CD8⁺T cells (E) were measured by flow cytometric analysis. **(F)** C57BL/6 mice ($n = 5$) were inoculated with 5×10^5 MC38 cells. Tumor-bearing mice were intraperitoneally treated with PBS or 30 μg $\alpha\text{PD-1-IL-15-R}$ on days 14, 17, and 20. FTY720 was intraperitoneally injected at 25 μg 1 d before the first treatment and 20 μg every other day to block T cells from exiting LNs. Tumor volume was measured as indicated. **(G)** C57BL/6 mice ($n = 10$) were inoculated with 8×10^5 MC38-OVA cells. Tumor-bearing mice were intratumorally treated with PBS or 30 μg $\alpha\text{PD-1-IL-15-R}$ on days 14 and 17. The mice were sacrificed and tumor tissues were collected 48 h after the second injection. The number of OVA-specific CD8⁺T cells was measured by H-2Kb-OVA257-264 tetramer flow cytometric staining. **(H)** Tetramer^{-/-} TILs were sorted from MC38-OVA tumor-bearing mice. 2×10^5 cells were incubated with PBS or 1 $\mu\text{g}/\text{ml}$ fusion proteins as indicated in vitro at 37°C for 24 h. IFN- γ in the supernatant was detected by a cytometric bead assay. **(I–K)** C57BL/6 mice were inoculated with 5×10^5 MC38 cells. Tumor-bearing mice were intratumorally treated with PBS or 30 μg $\alpha\text{PD-1-IL-15-R}$ on days 14 and 17. The mice were sacrificed, and tumor tissues were collected 48 h after the second injection. CD8⁺T cells were sorted for RNA-seq. Gene set enrichment analysis of T cell differentiation, T cell activation, and cytotoxic activity after $\alpha\text{PD-1-IL-15-R}$ treatment (I). ES, enrichment score; FDR, false discovery rate; NES, normalized enrichment score. *Gzmb*, *Prf1*, *Pdcd1*, *Il2rb* (K), and other gene expression levels (J) were shown. RC, read count. Data are shown as mean \pm SEM from two to three independent experiments. The P value was determined by two-way ANOVA with Geisser–Greenhouse’s correction (A–D and H) or two-tailed unpaired *t* test (E–G and K). **P* < 0.05, ***P* < 0.01, ****P* < 0.001, *****P* < 0.0001.

tumor cells 1 d before the treatment to mimic in situ and metastatic tumor model. The local tumor control and the decreased colony number in the lung indicated that $\alpha\text{PD-1-IL-15-R}$ could effectively control tumor metastasis (Fig. 5, D and E).

To study if neoadjuvant treatment could benefit from pre-surgical treatment of $\alpha\text{PD-1-IL-15-R}$ to reduce spontaneous metastasis, we used 4T1 mammary carcinoma, which is poor-immunogenic and can spontaneously metastasize 10 d after local tumor implantation. Mice-bearing established 4T1 tumors were treated with $\alpha\text{PD-1-IL-15-R}$, and the local tumor was resected after the treatment. The mouse survival curve indicated that $\alpha\text{PD-1-IL-15-R}$ treatment significantly prolonged survival, while the mice could not survive if treated with surgery or $\alpha\text{PD-1-IL-15-R}$ only (Fig. 5 F). These data demonstrated that $\alpha\text{PD-1-IL-15-R}$ could effectively control local tumor as well as lung metastasis and prolong mouse survival.

To renavigate IL-15 to intratumoral PD-1⁺CD8⁺T cells and reduce its toxicity, we engineered a PD-1–targeted concealed sIL-15 ($\alpha\text{PD-1-IL-15-R}$). The affinity of sIL-15 could be delicately adjusted through the length of linkers between Fc and IL-15. IL-15-R abrogated peripheral binding to NK cells and was re-navigated by $\alpha\text{PD-1}$ to intratumoral PD-1⁺CD8⁺T cells. In this case, $\alpha\text{PD-1-IL-15-R}$ could greatly reduce peripheral consumption and increase tumor retention. Most importantly, with the help of $\alpha\text{PD-1}$, the activity of IL-15-R could be fully restored through cis-delivery. Systematic injection of $\alpha\text{PD-1-IL-15-R}$ elicited potent antitumor immunity with negligible toxicity. The $\alpha\text{PD-1-IL-15-R}$ primarily expanded tumor-specific CD8⁺T cells in the tumor. Importantly, $\alpha\text{PD-1-IL-15-R}$ can control metastatic tumors and provide long-term protection. Altogether, $\alpha\text{PD-1-IL-15-R}$ offers a new strategy for next-generation cytokine application to take advantage of the antibody structure, which physically interrupts peripheral IL-15R β binding and cis-delivers sIL-15 to TILs.

Several recent studies have focused on generating low-affinity cytokine through mutations (Ren et al., 2022; Shen et al., 2020; Xu et al., 2021). Pfizer published an article with an $\alpha\text{PD-1-IL-15}$ fusion protein constructed by linking mutant IL-15 alone at the C terminal of $\alpha\text{PD-1}$ antibody and reducing its affinity with all the receptors (IL-15R α , IL-15R β , γ_c ; Xu et al., 2021). While mutations can reduce the affinity of cytokines to

their receptors, they might also increase the immunogenicity of cytokines, destabilize cytokines, and even lose IL-15 activity significantly. We took advantage of the high expression level of PD-1 in CD8⁺T cells over NK cells and used an $\alpha\text{PD-1}$ antibody to directly anchor the concealed sIL-15 on PD-1⁺CD8⁺T cells preferentially within the tumor. It is reported that most of these cells are tumor-primed active T cells. Only when targeted and anchored on the intratumoral PD-1⁺CD8⁺T cells by $\alpha\text{PD-1}$ could $\alpha\text{PD-1-IL-15-R}$ in cis deliver IL-15 signaling via IL-15R β receptor. $\alpha\text{PD-1}$ might also release PD-1 inhibition and promote cytotoxic function rather than exhaustion for CTLs by synergizing with IL-15. Eventually, we observed that $\alpha\text{PD-1-IL-15-R}$ could release the PD-1/PD-L1 inhibition and promote CD8⁺T cells’ function, which significantly enhanced antitumor immunity and overcame the resistance of ICB.

Many molecules (such as EGFR, PD-L1, Claudin18.2, etc.) are highly expressed on tumor cells and used for cytokine tumor-targeting, but these targets are not available for cis-delivery onto the TILs. Intriguingly, cis-delivery of $\alpha\text{PD-1-IL-15-R}$ would allow sIL-15 to retain and function on tumor-reactive PD-1 high CD8⁺T cells instead of PD-1 low/negative cells. We found that the length of linkers between Fc and IL-15 can be applied to adjust its efficacy versus toxicity precisely, as the longer linkers will have more potent activity and visible toxicity. We used the αEGFR antibody as an effective target for the MC38-EGFR5 tumor model to deliver IL-15-R, which displayed limited tumor control, while IL-15-R activity could be fully recovered when $\alpha\text{PD-1-IL-15-R}$ was used. This phenomenon also confirms our cis-delivery model in which $\alpha\text{PD-1-IL-15-R}$ could only function on PD-1⁺IL-15R β ⁺ cells. There are some limitations of this study: (1) It is unclear if the cis-delivery of concealed IL-15 could also be applied to other T cell cosignals on TILs. (2) It remains to be determined if PD-1 blockade at this low dose is required to synergize with IL-15.

A previous study has provided several ways to select an appropriate target for cytokine delivery, which should be highly expressed on TILs and be sensitive to cytokine accessibility (Ren et al., 2022). Thus, our study provides an alternative way for antibody–cytokine fusion protein: (a) Cytokine should be carefully chosen to limit the receptor binding site with low freedom in the periphery; (b) Fc domain is subtly used to conceal the

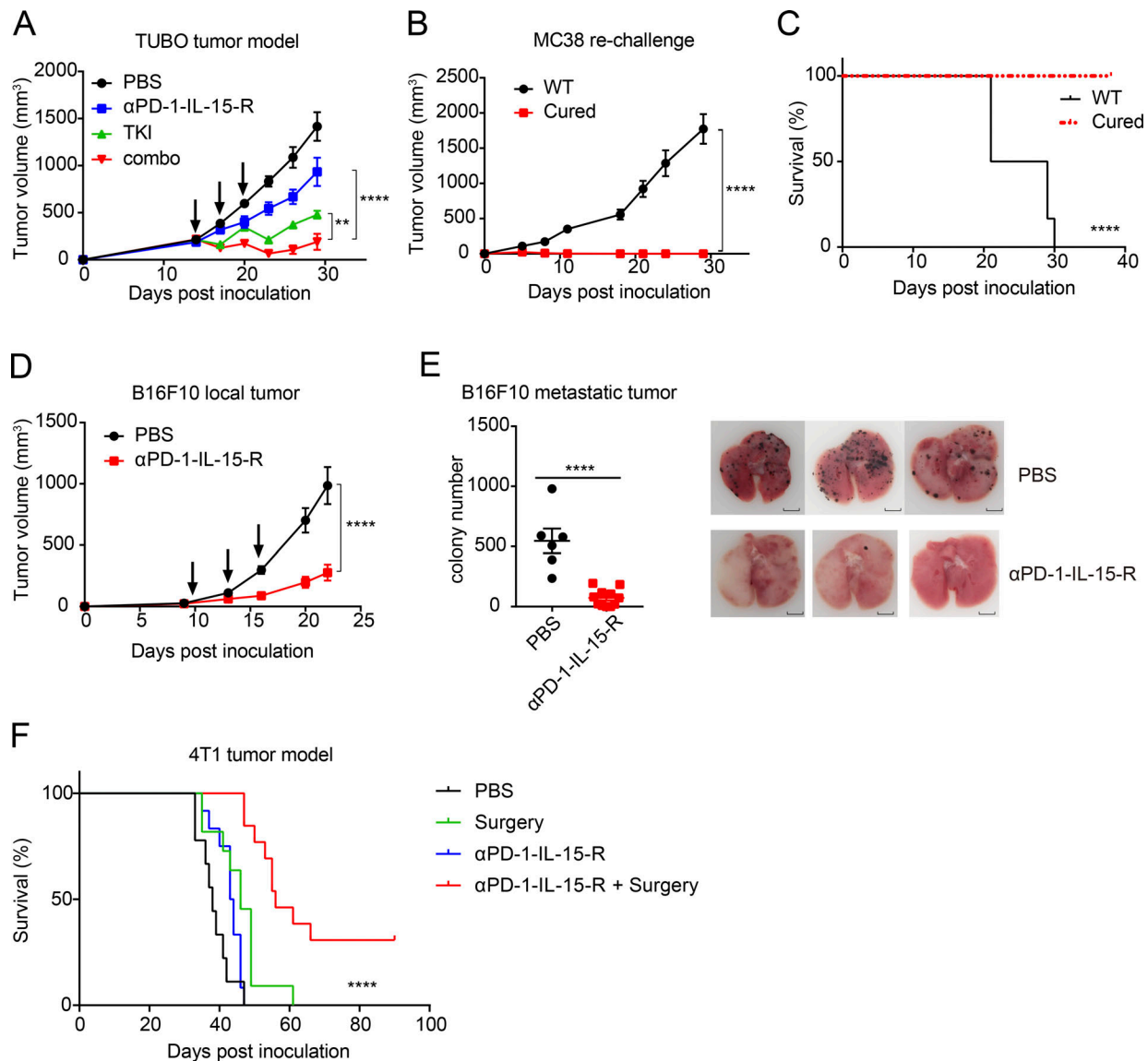


Figure 5. α PD-1-IL-15-R controls cold tumor and metastatic tumor. (A) Balb/c mice ($n = 5$) were subcutaneously inoculated with 5×10^5 TUBO cells. Tumor-bearing mice were intraperitoneally treated with $30 \mu\text{g}$ α PD-1-IL-15 on days 14, 17, and 20. TKI (Afatinib, 1 mg) was orally administered on days 14 and 20. Tumor volume was measured as indicated. (B and C) Naive mice ($n = 5$) or mice with complete tumor regression ($n = 10$) were re-challenged with 3×10^6 MC38 cells. Tumor volume (B) and survival (C) were measured as indicated. (D and E) C57BL/6 mice ($n = 6$ –11) were inoculated with 3×10^5 B16F10 cells. 3×10^5 B16F10 cells were intravenously inoculated on day 9. Tumor-bearing mice were intratumorally treated with PBS or $30 \mu\text{g}$ α PD-1-IL-15-R on days 10, 13, and 16. The local tumor was measured as indicated. The mice were sacrificed on day 20. The colony number on the lung was counted (scale bar: $100 \mu\text{m}$). (F) Balb/c mice ($n = 9$ –12) were inoculated with 1.5×10^5 4T1 cells. Tumor-bearing mice were intraperitoneally treated with PBS or $30 \mu\text{g}$ α PD-1-IL-15-R on days 8 and 11. The primary tumors were resected on day 15. The survival curve was measured. Data are shown as mean \pm SEM from two to three independent experiments. The P value was determined by two-way ANOVA with Geisser–Greenhouse’s correction (A, B, and D) or two-tailed unpaired t test (E) or a log-rank test (C and F). ** $P < 0.01$, **** $P < 0.0001$.

essential binding site with a proper orientation; (c) antibody should cis-deliver the concealed-cytokine to the effector cells, and Fab format is powerful than single-chain variable fragment for the effective target (Crivianu-Gaita and Thompson, 2016); (d) antitumor effects are more potent when the antibody has positive function synergized with cytokine such as releasing the inhibition or reshaping immunosuppressive TME; (e) cytokine format should be potent after interaction with effector cells to provide substantial tumor control.

Overall, our α PD-1-IL-15-R offers a new strategy for next-generation cytokines application. Instead of mutation, α PD-1-IL-15-R takes advantage of the antibody structure to interrupt peripheral IL-15R β binding physically and cis-delivers sIL-15 to TILs. The simultaneous expansion and activation of tumor-specific CD8 $^+$ T cells result in dramatic local and metastatic tumor regression. Hence, α PD-1-IL-15-R could be used to overcome the current dilemma of cytokine application and provides a valuable basis for clinical translation.

Materials and methods

Mice

6–8-wk old WT BALB/c and C57BL/6j female mice were purchased from SPF Biotechnology. *Rag1*^{-/-} mice were purchased from the Model Animal Research Center of Nanjing University. All mice were maintained under specific pathogen-free conditions.

Cell lines and reagents

A20, MC38, B16F10, 4T1, 293T, and CTLL-2 were purchased from the American Type Culture Collection. MC38-OVA was selected from signal-cell clone after transfection by lentivirus-expressed OVA. TUBO was cloned from a spontaneous mammary tumor in BALB/c *Neu*-transgenic mice. Freestyle 293-F (R79007) was purchased from Invitrogen. All cell lines were routinely tested for mycoplasma contamination. A20, 4T1, and TUBO were cultured in RPMI 1640 with 10% heat-inactivated fetal bovine serum, 2 mmol/liter *L*-glutamine, 100 U/ml penicillin-streptomycin under 5% CO₂ at 37°C. CTLL-2 was cultured in RPMI 1640 with established protocol. MC38, B16F10, 293T, and MC38-OVA were cultured in Dulbecco's modified Eagle's medium with 10% heat-inactivated fetal bovine serum, 2 mmol/liter *L*-glutamine, 100 U/ml penicillin-streptomycin under 5% CO₂ at 37°C. 293-F was cultured in SMM 293-TI medium (M293TI; Sino Biological).

α PD-L1 antibody (10F.9G2) and anti-IL-15R β (TM- β 1) were purchased from Bio X Cell. FTY720 was purchased from Sigma-Aldrich. TKI-Afatinib was purchased from Shanghai Bojing Chemical Company. Anti-CD8 antibody (TIB210), anti-CD4 antibody (GK1.5), anti-NK1.1 antibody (PK136), and Fc γ RII/III blocking antibody (2.4G2) were produced in-house. α PD-1-IL-15-R or α PD-1-R-IL-15 were cloned into a pEE12.4 vector and transfected into 293-F cells. The supernatant was purified by Protein-A affinity chromatography (GE Healthcare) according to the established protocol.

CTLL-2-mPD-1 cell line engineering

Lentivirus was produced by transient transfection of 293T cells. The plasmids of psPAX2, pMD2.G, and pSin-EF2-mouse PD-1 at the ratio of 4:2:3 were mixed with Lipofectamine 300 reagent (Thermo Fisher Scientific) by established protocol. The lentivirus in the media was harvested 48 h later and filtered through a 0.45- μ m filter. The original CTLL-2 cells were transduced with lentivirus expressing the extracellular domain of PD-1 for 48 h. CTLL-2-mPD-1 cells were stained and selected by BD Aria III (BD Biosciences).

Tumor growth and treatment

A20 cells (5×10^6), MC38 cells ($3\text{--}5 \times 10^5$), B16F10 cells (3×10^5), MC38-OVA cells (8×10^5), and TUBO cells (5×10^5) were subcutaneously injected into the right flank of BALB/c or C57BL/6j mice. 4T1 cells (1.5×10^5) were injected into the mammary fat pad. The tumor volume was measured twice a week and calculated as length \times width \times height/2. The mice were treated with PBS and 30 μ g α PD-1-IL-15-R, α PD-1-R-IL-15, or α EGFR-IL-15-R. 200 μ g anti-CD8 antibody, 200 μ g anti-CD4 antibody, 200 μ g anti-IL-15R β , or 400 μ g anti-NK1.1 antibody was injected

intraperitoneally every 3 d. 25 μ g FTY720 was injected intraperitoneally for the first time and 20 μ g every other day to maintain the blockade. 1 mg TKI was treated orally every 5 d for a total of two doses.

Flow cytometry

Tumor tissues were collected and digested with 1 mg/ml collagenase IV (Roche) and 100 μ g/ml DNase I (Roche) at 37°C for 40 min. Single-cell suspensions of cells were incubated with Fc γ RII/III blocking antibody (2.4G2) and stained with specific antibodies followed by established protocol. Samples were analyzed or isolated on BD LSR Fortessa or BD Aria III (BD Biosciences). Data were analyzed by FlowJo software (Treestar).

RNA-seq

TILs were isolated from MC38 tumor-bearing mice 48 h after the second injection of α PD-1-IL-15-R. Total RNA extraction, mRNA library construction, and sequencing were established by BGI. The clean reads were mapped to the genome using HISAT2 (v2.0.4). The expression level of a gene was calculated by RSEM (v1.2.12). The mRNA expression level (calculated from transcripts per million, or $\log_{10}[\text{TPM}+1]$) was calculated and the heat map was generated in R (v3.5.1) using a pheatmap (v1.0.10). Raw data have been uploaded to Gene Expression Omnibus, National Center for Biotechnology Information (accession number GSE212545).

Statistics

Data are shown as the mean \pm SEM or SD. Statistical analysis were performed by GraphPad Software. Statistically significant differences of $P < 0.05$, $P < 0.01$, $P < 0.001$, and $P < 0.0001$ are noted with *, **, *** and ****.

Study approval

Animal experiment protocols and studies were approved by the Animal Care and Use Committee of Chinese Academy of Sciences.

Online supplemental material

Fig. S1 shows that IL-15-R peripheral toxicity was abolished by concealing IL-15R β binding. Fig. S2 shows that α PD-1 rather than α PD-L1 targeting enhanced IL-15-R bioactivity. Fig. S3 shows that α PD-1-IL-15-R antitumor activity depended on the proliferation of the reinvigorated intratumoral CD8⁺T cells.

Acknowledgments

The authors thank all lab members and Yuchen He for the discussion, professor Pu Gao for the consult of protein structures, and the support from the animal facility of the Institute of Biophysics, Chinese Academy of Sciences, especially Xiang Shi and Chunyan Lv for assistance.

This work was supported by funding from the Chinese Academy of Sciences (KFJ-STZ-ZDTP-062 and XDA12020212) to H. Peng and National Key S&T Special project of China (2018ZX1030140402) to H. Peng.

Author contributions: Conceptualization: J. Shen, H. Peng, and Y.-X. Fu; Methodology: J. Shen, Z. Zou, J. Guo, Y. Cai, D. Xue, Y. Liang, and W. Wang; Investigation: J. Shen and Z. Zou; Formal analysis: J. Shen, Z. Zou, H. Peng, and Y.-X. Fu; Writing—Original Draft: J. Shen; Writing—Review & Editing: J. Shen, Z. Zou, H. Peng, and Y.-X. Fu; Supervision: H. Peng and Y.-X. Fu.

Disclosures: H. Peng reported a patent to “construction and application of IL-15 based fusion proteins” pending. No other disclosures were reported.

Submitted: 29 April 2022

Revised: 15 August 2022

Accepted: 8 September 2022

References

- Beha, N., M. Harder, S. Ring, R.E. Kontermann, and D. Muller. 2019. IL15-Based trifunctional antibody-fusion proteins with costimulatory TNF-superfamily ligands in the single-chain format for cancer immunotherapy. *Mol. Cancer Ther.* 18:1278–1288. <https://doi.org/10.1158/1535-7163.MCT-18-1204>
- Brahmer, J.R., S.S. Tykodi, L.Q.M. Chow, W.-J. Hwu, S.L. Topalian, P. Hwu, C.G. Drake, L.H. Camacho, J. Kauh, K. Odunsi, et al. 2012. Safety and activity of anti-PD-L1 antibody in patients with advanced cancer. *N. Engl. J. Med.* 366:2455–2465. <https://doi.org/10.1056/NEJMoa1200694>
- Crivianu-Gaita, V., and M. Thompson. 2016. Aptamers, antibody scFv, and antibody Fab' fragments: An overview and comparison of three of the most versatile biosensor biorecognition elements. *Biosens. Bioelectron.* 85:32–45. <https://doi.org/10.1016/j.bios.2016.04.091>
- Ellis-Connell, A.L., A.J. Balgeman, K.R. Zarbock, G. Barry, A. Weiler, J.O. Egan, E.K. Jeng, T. Friedrich, J.S. Miller, A.T. Haase, et al. 2018. ALT-803 transiently reduces simian immunodeficiency virus replication in the absence of antiretroviral treatment. *J. Virol.* 92:e01748–17. <https://doi.org/10.1128/JVI.01748-17>
- Fiore, P.F., S. Di Matteo, N. Tumino, F.R. Mariotti, G. Pietra, S. Ottonello, S. Negrini, B. Bottazzi, L. Moretta, E. Mortier, and B. Azzarone. 2020. Interleukin-15 and cancer: Some solved and many unsolved questions. *J. Immunother. Cancer.* 8:e001428. <https://doi.org/10.1136/jitc-2020-001428>
- Garris, C.S., S.P. Arlauckas, R.H. Kohler, M.P. Trefny, S. Garren, C. Piot, C. Engblom, C. Pfirschke, M. Siwicki, J. Gungabeesoon, et al. 2018. Successful anti-PD-1 cancer immunotherapy requires T cell-dendritic cell crosstalk involving the cytokines IFN- γ and IL-12. *Immunity.* 49:1148–1161.e7. <https://doi.org/10.1016/j.immuni.2018.09.024>
- Guo, J., Y. Liang, D. Xue, J. Shen, Y. Cai, J. Zhu, Y.X. Fu, and H. Peng. 2021. Tumor-conditional IL-15 pro-cytokine reactivates anti-tumor immunity with limited toxicity. *Cell Res.* 31:1190–1198. <https://doi.org/10.1038/s41422-021-00543-4>
- Hannani, D., M. Vetizou, D. Enot, S. Rusakiewicz, N. Chaput, D. Klatzmann, M. Desbois, N. Jacquilot, N. Vimond, S. Chouaib, et al. 2015. Anticancer immunotherapy by CTLA-4 blockade: Obligatory contribution of IL-2 receptors and negative prognostic impact of soluble CD25. *Cell Res.* 25:208–224. <https://doi.org/10.1038/cr.2015.3>
- Huang, A.C., M.A. Postow, R.J. Orlowski, R. Mick, B. Bensch, S. Manne, W. Xu, S. Harmon, J.R. Giles, B. Wenz, et al. 2017. T-cell invigoration to tumour burden ratio associated with anti-PD-1 response. *Nature.* 545:60–65. <https://doi.org/10.1038/nature22079>
- Jochems, C., S.R. Tritsch, K.M. Knudson, S.R. Gameiro, C. Smalley Rumfield, S.T. Pellom, Y.M. Morillon, R. Newman, W. Marcus, C. Szeto, et al. 2019. The multi-functionality of N-809, a novel fusion protein encompassing anti-PD-L1 and the IL-15 superagonist fusion complex. *Oncoimmunology.* 8:e1532764. <https://doi.org/10.1080/2162402X.2018.1532764>
- Knudson, K.M., K.C. Hicks, Y. Ozawa, J. Schlom, and S.R. Gameiro. 2020. Functional and mechanistic advantage of the use of a bifunctional anti-PD-L1/IL-15 superagonist. *J. Immunother. Cancer.* 8:e000493. <https://doi.org/10.1136/jitc-2019-000493>
- Lenardo, M.J. 1996. Fas and the art of lymphocyte maintenance. *J. Exp. Med.* 183:721–724. <https://doi.org/10.1084/jem.183.3.721>
- Liu, B., P. Chaturvedi, M. Wang, X. Zhu, V. George, K. Revelo, C. Spanoudis, L. Kong, J. Xing, C. Prendes, et al. 2020. A novel bifunctional fusion protein comprising of TGF- β RII trap and IL15/IL-15R α as an immunotherapeutic against cancer. *J. Immunol.* 204:90
- Liu, Y., Y. Wang, J. Xing, Y. Li, J. Liu, and Z. Wang. 2018. A novel multi-functional anti-CEA-IL15 molecule displays potent antitumor activities. *Drug Des. Dev. Ther.* 12:2645–2654. <https://doi.org/10.2147/DDDT.S166373>
- Liu, Y., N. Zhou, L. Zhou, J. Wang, Y. Zhou, T. Zhang, Y. Fang, J. Deng, Y. Gao, X. Liang, et al. 2021. IL-2 regulates tumor-reactive CD8(+) T cell exhaustion by activating the aryl hydrocarbon receptor. *Nat. Immunol.* 22:358–369. <https://doi.org/10.1038/s41590-020-00850-9>
- Margolin, K., C. Morishima, V. Velcheti, J.S. Miller, S.M. Lee, A.W. Silk, S.G. Holtan, A.M. Lacroix, S.P. Fling, J.C. Kaiser, et al. 2018. Phase I trial of ALT-803, A novel recombinant IL15 complex, in patients with advanced solid tumors. *Clin. Cancer Res.* 24:5552–5561. <https://doi.org/10.1158/1078-0432.CCR-18-0945>
- Martomo, S.A., D. Lu, Z. Polonskaya, X. Luna, Z. Zhang, S. Feldstein, R. Lumban-Tobing, D.K. Almstead, F. Miyara, and J. Patel. 2020. Single-dose anti-PD-L1/IL-15 fusion protein KD033 generates synergistic anti-tumor immunity with robust tumor-immune gene signatures and memory responses. *Mol. Cancer Ther.* 20:347–356. <https://doi.org/10.1158/1535-7163.MCT-20-0457>
- Miller, B.C., D.R. Sen, R. Al Abosy, K. Bi, Y.V. Virkud, M.W. LaFleur, K.B. Yates, A. Lako, K. Felt, G.S. Naik, et al. 2019. Subsets of exhausted CD8(+) T cells differentially mediate tumor control and respond to checkpoint blockade. *Nat. Immunol.* 20:326–336. <https://doi.org/10.1038/s41590-019-0312-6>
- Mlecnik, B., G. Bindea, H.K. Angell, M.S. Sasso, A.C. Obenaus, T. Fredriksen, L. Lafontaine, A.M. Bilocq, A. Kirilovsky, M. Tosolini, et al. 2014. Functional network pipeline reveals genetic determinants associated with in situ lymphocyte proliferation and survival of cancer patients. *Sci. Transl. Med.* 6:228ra37. <https://doi.org/10.1126/scitranslmed.3007240>
- Ochoa, M.C., J. Fioravanti, I. Rodriguez, S. Hervas-Stubbis, A. Azpilikueta, G. Mazzolini, A. Gurpide, J. Prieto, J. Pardo, P. Bertraondo, and I. Melero. 2013. Antitumor immunotherapeutic and toxic properties of an HDL-conjugated chimeric IL-15 fusion protein. *Cancer Res.* 73:139–149. <https://doi.org/10.1158/0008-5472.CAN-12-2660>
- Ren, Z., A. Zhang, Z. Sun, Y. Liang, J. Ye, J. Qiao, B. Li, and Y.X. Fu. 2022. Selective delivery of low-affinity IL-2 to PD-1⁺ T cells rejuvenates antitumor immunity with reduced toxicity. *J. Clin. Invest.* 132:e153604. <https://doi.org/10.1172/JCI153604>
- Rhode, P.R., J.O. Egan, W. Xu, H. Hong, G.M. Webb, X. Chen, B. Liu, X. Zhu, J. Wen, L. You, et al. 2016. Comparison of the superagonist complex, ALT-803, to IL15 as cancer immunotherapeutics in animal models. *Cancer Immunol. Res.* 4:49–60. <https://doi.org/10.1158/2326-6066.CIR-15-0093-T>
- Ring, A.M., J.-X. Lin, D. Feng, S. Mitra, M. Rickert, G.R. Bowman, V.S. Pande, P. Li, I. Moraga, R. Spolski, et al. 2012. Mechanistic and structural insight into the functional dichotomy between IL-2 and IL-15. *Nat. Immunol.* 13:1187–1195. <https://doi.org/10.1038/ni.2449>
- Robinson, T.O., and K.S. Schluns. 2017. The potential and promise of IL-15 in immuno-oncogenic therapies. *Immunol. Lett.* 190:159–168. <https://doi.org/10.1016/j.imlet.2017.08.010>
- Romee, R., S. Cooley, M.M. Berrien-Elliott, P. Westervelt, M.R. Verneris, J.E. Wagner, D.J. Weisdorf, B.R. Blazar, C. Ustun, T.E. DeFor, et al. 2018. First-in-human phase 1 clinical study of the IL-15 superagonist complex ALT-803 to treat relapse after transplantation. *Blood.* 131:2515–2527. <https://doi.org/10.1182/blood-2017-12-823757>
- Rosenberg, S.A. 2014. IL-2: The first effective immunotherapy for human cancer. *J. Immunol.* 192:5451–5458. <https://doi.org/10.4049/jimmunol.1490019>
- Rubinstein, M.P., M. Kovar, J.F. Purton, J.-H. Cho, O. Boyman, C.D. Surh, and J. Sprent. 2006. Converting IL-15 to a superagonist by binding to soluble IL-15R α . *Proc. Natl. Acad. Sci. USA.* 103:9166–9171. <https://doi.org/10.1073/pnas.0600240103>
- Sakuishi, K., L. Apetoh, J.M. Sullivan, B.R. Blazar, V.K. Kuchroo, and A.C. Anderson. 2010. Targeting Tim-3 and PD-1 pathways to reverse T cell exhaustion and restore anti-tumor immunity. *J. Exp. Med.* 207:2187–2194. <https://doi.org/10.1084/jem.20100643>
- Santana Carrero, R.M., F. Beceren-Braun, S.C. Rivas, S.M. Hegde, A. Gangadharan, D. Plote, G. Pham, S.M. Anthony, and K.S. Schluns. 2019. IL-15 is a component of the inflammatory milieu in the tumor microenvironment promoting antitumor responses. *Proc. Natl. Acad. Sci. USA.* 116:599–608. <https://doi.org/10.1073/pnas.1814642116>
- Scott, A.M., J.D. Wolchok, and L.J. Old. 2012. Antibody therapy of cancer. *Nat. Rev. Cancer.* 12:278–287. <https://doi.org/10.1038/nrc3236>

- Sharpe, A.H., and K.E. Pauken. 2018. The diverse functions of the PD1 inhibitory pathway. *Nat. Rev. Immunol.* 18:153–167. <https://doi.org/10.1038/nri.2017.108>
- Shen, S., G. Sckisel, A. Sahoo, A. Lalani, D.D. Otter, J. Pearson, J. DeVoss, J. Cheng, S.C. Casey, R. Case, et al. 2020. Engineered IL-21 cytokine mutants fused to anti-PD-1 antibodies can improve CD8⁺ T cell function and anti-tumor immunity. *Front. Immunol.* 11:832. <https://doi.org/10.3389/fimmu.2020.00832>
- Stoklasek, T.A., K.S. Schluns, and L. Lefrancois. 2006. Combined IL-15/IL-15R α immunotherapy maximizes IL-15 activity in vivo. *J. Immunol.* 177:6072–6080. <https://doi.org/10.4049/jimmunol.177.9.6072>
- Tang, H., Y. Liang, R.A. Anders, J.M. Taube, X. Qiu, A. Mulgaonkar, X. Liu, S.M. Harrington, J. Guo, Y. Xin, et al. 2018. PD-L1 on host cells is essential for PD-L1 blockade-mediated tumor regression. *J. Clin. Invest.* 128:580–588. <https://doi.org/10.1172/JCI96061>
- Thommen, D.S., and T.N. Schumacher. 2018. T cell dysfunction in cancer. *Cancer Cell.* 33:547–562. <https://doi.org/10.1016/j.ccell.2018.03.012>
- Topalian, S.L., F.S. Hodi, J.R. Brahmer, S.N. Gettinger, D.C. Smith, D.F. McDermott, J.D. Powderly, R.D. Carvajal, J.A. Sosman, M.B. Atkins, et al. 2012. Safety, activity, and immune correlates of anti-PD-1 antibody in cancer. *N. Engl. J. Med.* 366:2443–2454. <https://doi.org/10.1056/NEJMoa1200690>
- Vilain, R.E., A.M. Menzies, J.S. Wilmott, H. Kakavand, J. Madore, A. Guminiski, E. Liniker, B.Y. Kong, A.J. Cooper, J.R. Howle, et al. 2017. Dynamic changes in PD-L1 expression and immune infiltrates early during treatment predict response to PD-1 blockade in melanoma. *Clin. Cancer Res.* 23:5024–5033. <https://doi.org/10.1158/1078-0432.CCR-16-0698>
- Vincent, M., A. Bessard, D. Cochonneau, G. Teppaz, V. Sole, M. Maillason, S. Birkle, L. Garrigue-Antar, A. Quemener, and Y. Jacques. 2013. Tumor targeting of the IL-15 superagonist RLI by an anti-GD2 antibody strongly enhances its antitumor potency. *Int. J. Cancer.* 133:757–765. <https://doi.org/10.1002/ijc.28059>
- Waldmann, T.A., S. Dubois, M.D. Miljkovic, and K.C. Conlon. 2020. IL-15 in the combination immunotherapy of cancer. *Front. Immunol.* 11:868. <https://doi.org/10.3389/fimmu.2020.00868>
- West, E.E., H.T. Jin, A.U. Rasheed, P. Penaloza-Macmaster, S.J. Ha, W.G. Tan, B. Youngblood, G.J. Freeman, K.A. Smith, and R. Ahmed. 2013. PD-L1 blockade synergizes with IL-2 therapy in reinvigorating exhausted T cells. *J. Clin. Invest.* 123:2604–2615. <https://doi.org/10.1172/JCI67008>
- Wrangle, J.M., V. Velcheti, M.R. Patel, E. Garrett-Mayer, E.G. Hill, J.G. Ravenel, J.S. Miller, M. Farhad, K. Anderton, K. Lindsey, et al. 2018. ALT-803, an IL-15 superagonist, in combination with nivolumab in patients with metastatic non-small cell lung cancer: A non-randomised, open-label, phase 1b trial. *Lancet Oncol.* 19:694–704. [https://doi.org/10.1016/S1470-2045\(18\)30148-7](https://doi.org/10.1016/S1470-2045(18)30148-7)
- Xu, Y., L.C. Carrascosa, Y.A. Yeung, M.L.H. Chu, W. Yang, I. Djuretic, D.C. Pappas, J. Zeytounian, Z. Ge, V. de Ruiter, et al. 2021. An engineered IL15 cytokine mutein fused to an anti-PD1 improves intratumoral T-cell function and antitumor immunity. *Cancer Immunol. Res.* 9:1141–1157. <https://doi.org/10.1158/2326-6066.CIR-21-0058>
- Xue, D., E. Hsu, Y.-X. Fu, and H. Peng. 2021. Next-generation cytokines for cancer immunotherapy. *Antibody Ther.* 4:123–133. <https://doi.org/10.1093/abt/tbab014>

Supplemental material

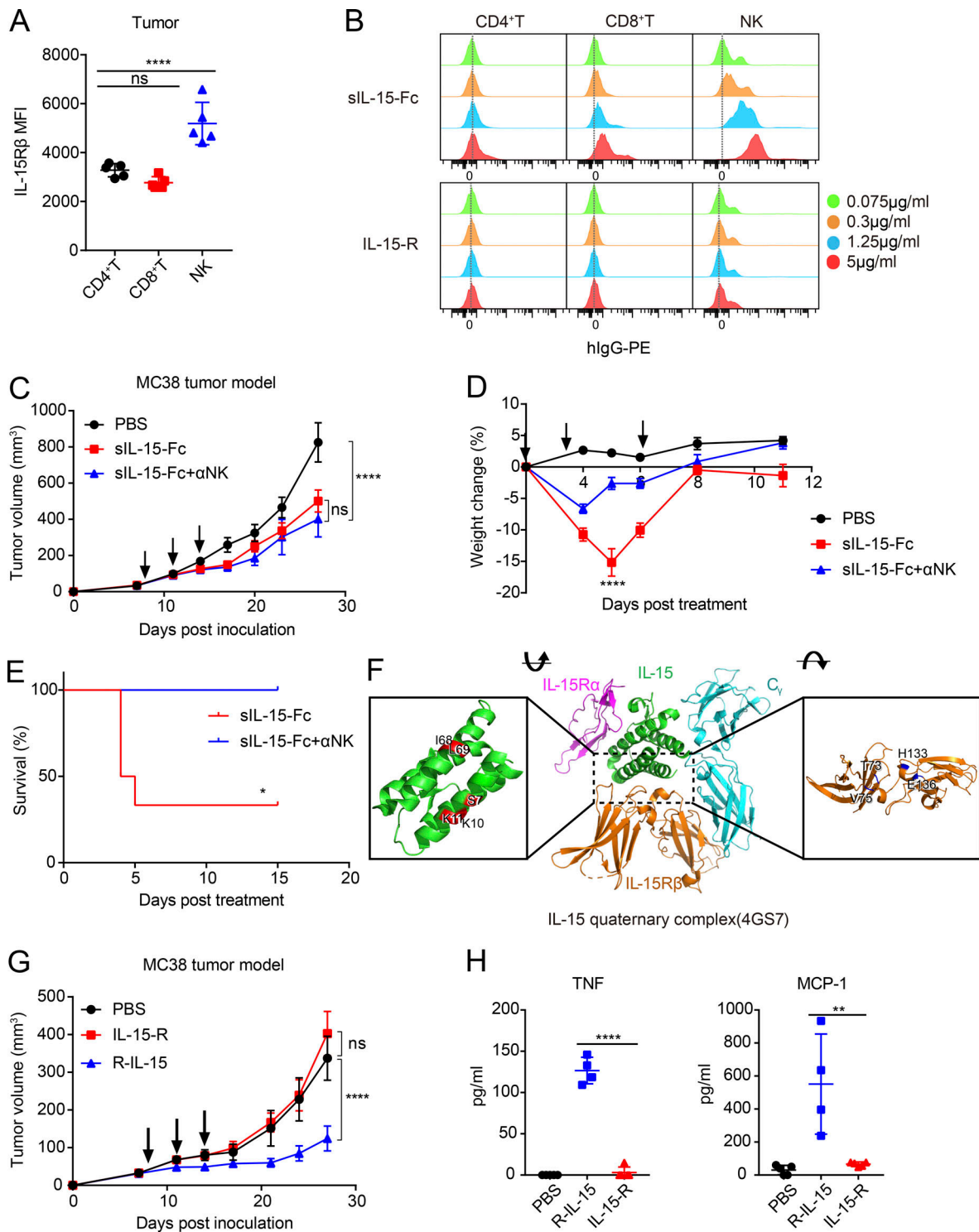


Figure S1. **IL-15-R peripheral toxicity was abolished by concealing IL-15R β binding.** (A) Tumors were collected from tumor-bearing mice 14 d after the inoculation. Certain cell types were isolated and stained for flow cytometric analysis. (B) sIL-15-Fc and IL-15-R were incubated with splenocytes in different concentrations. Protein binding with CD4⁺T, CD8⁺T, and NK cells was detected by flow cytometric analysis. (C–E) C57BL/6 mice ($n = 5$) were inoculated with 5×10^5 MC38 cells. Tumor-bearing mice were intravenously treated with PBS or 30 μ g sIL-15-Fc on days 8, 11, and 14. For cell depletion, mice were injected with 500 μ g of α NK1.1 antibody on the same day. Tumor volume (C), body weight (D), and survival (E) were measured as indicated. (F) The structure of the IL-15 quaternary complex (4GS7) was downloaded from The Protein Data Bank (<https://www.rcsb.org/>). Certain amino acids in the interface were labeled based on the publication of 4GS7. (G) C57BL/6 mice ($n = 5$) were inoculated with 5×10^5 MC38 cells. Tumor-bearing mice were intraperitoneally treated with PBS or 15 μ g IL-15-R or R-IL-15 on days 7, 10, and 13. Tumor volume was measured as indicated. (H) The mice were treated as shown in G. TNF and MCP-1 from the serum were measured 6 h after the second injection by a cytometric bead assay. Data are shown as mean \pm SEM from two to three independent experiments. The P value was determined by two-way ANOVA with Geisser–Greenhouse’s correction (A, C, D, G, and H) or a log-rank test (E). * $P < 0.05$, ** $P < 0.01$, **** $P < 0.0001$.

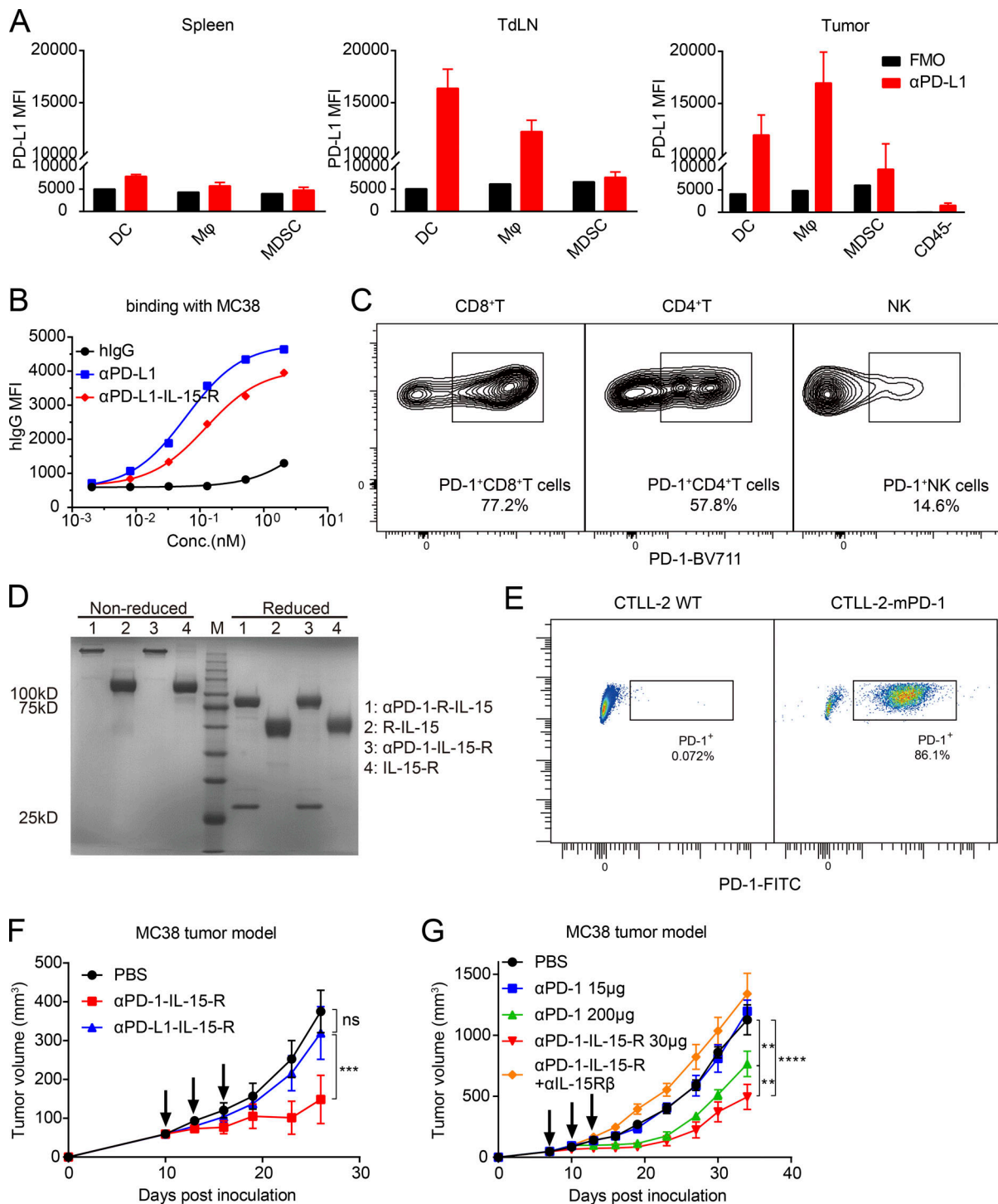


Figure S2. **αPD-1 rather than αPD-L1 targeting enhanced IL-15-R bioactivity.** (A) C57BL/6 mice were inoculated with 5×10^5 MC38 cells, and tissues (spleen, dLN, and tumor) were collected. The PD-L1 levels of DC, Mφ, and MDSCs from the indicated tissues were measured by flow cytometric analysis. (B) MC38 tumor cells were collected and incubated with different proteins as indicated. Protein binding with MC38 tumor cells was detected by flow cytometric analysis. (C) C57BL/6 mice were inoculated with 5×10^5 MC38 cells. PD-1 level of CD4⁺T, CD8⁺T, and NK cells from the tumor was measured by flow cytometric analysis. (D) Reduced and non-reduced SDS-PAGE analysis for the indicated proteins. (E) The CTLL-2-mPD-1 reporter cell line was derived from the original CTLL-2 cell line transduced by lentivirus expressing the extracellular domain of mouse PD-1. The PD-1 overexpression level of CTLL-2-mPD-1 cells was detected by flow cytometric analysis. (F) C57BL/6 mice ($n = 5$) were inoculated with 5×10^5 MC38 cells. Tumor-bearing mice were intraperitoneally treated with PBS or 30 μg αPD-1-IL-15-R or αPD-L1-IL-15-R on days 10, 13, and 16. Tumor volume was measured as indicated. (G) C57BL/6 mice ($n = 5$) were inoculated with 5×10^5 MC38 cells. Tumor-bearing mice were intraperitoneally treated with PBS or 15 μg/200 μg αPD-1 or 30 μg αPD-1-IL-15-R or 200 μg αIL-15Rβ on days 7, 10, and 13. Tumor volume was measured as indicated. Data are shown as mean \pm SEM from two to three independent experiments. The P value was determined by two-way ANOVA with Geisser–Greenhouse’s correction (F and G). MFI, mean fluorescence intensity. **P < 0.01, ***P < 0.001, ****P < 0.0001. Source data are available for this figure: SourceData FS2.

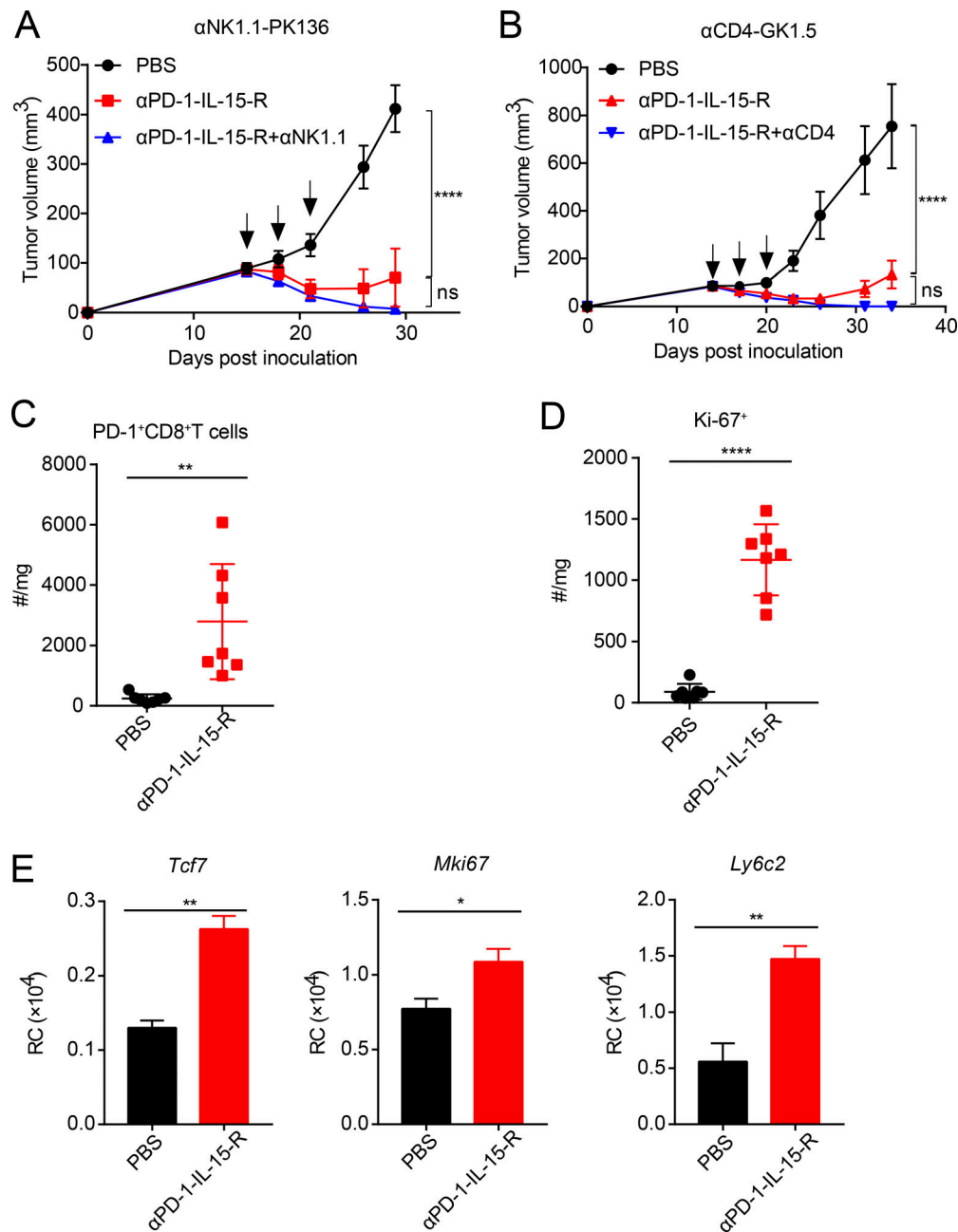


Figure S3. **α PD-1-IL-15-R antitumor activity depended on the proliferation of the reinvigorated intratumoral CD8⁺T cells.** (A and B) C57BL/6 mice ($n = 5$) were inoculated with 5×10^5 MC38 cells. Tumor-bearing mice were intraperitoneally treated with PBS or 30 μ g α PD-1-IL-15-R on days 14, 17, and 20. For cell depletion, mice were injected with 400 μ g α NK1.1 (A) or 200 μ g α CD4 (B) antibodies on the same day. Tumor volume was measured as indicated. (C and D) C57BL/6 mice ($n = 7$) were inoculated with 5×10^5 MC38 cells. Tumor-bearing mice were intratumorally treated with PBS or 30 μ g α PD-1-IL-15-R on days 14 and 17. The mice were sacrificed, and tumor tissues were collected 48 h after the second injection. The number of intratumoral PD-1⁺CD8⁺T cells (C) and Ki-67⁺PD-1⁺CD8⁺T cells (D) were measured by flow cytometric analysis. (E) C57BL/6 mice were inoculated with 5×10^5 MC38 cells. Tumor-bearing mice were intratumorally treated with PBS or 30 μ g α PD-1-IL-15-R on days 14 and 17. The mice were sacrificed, and tumor tissues were collected 48 h after the second injection. CD8⁺T cells were sorted for RNA-seq. The expression level of *Tcf7*, *Mki67*, and *Ly6c2* were shown. Data are shown as mean \pm SEM from two to three independent experiments. The P value was determined by two-way ANOVA with Geisser–Greenhouse’s correction (A and B) or two-tailed unpaired *t* test (C–E). * $P < 0.05$, ** $P < 0.01$, **** $P < 0.0001$. RC, read count.